Progress In Electromagnetics Research C, Vol. 19, 93–106, 2011

COMPACT THIRD-ORDER MICROSTRIP BANDPASS FILTER USING HYBRID RESONATORS

F. Xiao

The EHF Key Laboratory of Fundamental Science
School of Electronic Engineering
University of Electronic Science and Technology of China
Chengdu, Sichuan 610054, China

M. Norgren and S. He

Department of Electromagnetic Engineering
School of Electrical Engineering
KTH Royal Institute of Technology, Stockholm 10044, Sweden

Abstract—In this paper, a novel microwave bandpass filter structure is proposed. By introducing a metallic via hole, the filter structure operates as one $\lambda/2$ and two $\lambda/4$ uniform impedance resonators and consequently form a triplet coupling scheme. The equivalent circuit model is analyzed in detail, which shows that there is a transmission zero in the low stopband. Based on that concept, three microstrip filters are designed, fabricated and measured, respectively. The first filter has no source/load coupling and only one transmission zero is created. By introducing source/load coupling, the second filter can create three transmission zeros. The third filter can create a controllable transmission zero in upper stopband. The simulated and measured results agree very well.

1. INTRODUCTION

Microwave filters have found wide applications in various RF/microwave circuits and systems. Planar microwave filters are particularly popular because they can be fabricated by using printed circuit technology and are suitable for commercial applications due to their compact size

Received 27 September 2010, Accepted 27 December 2010, Scheduled 15 January 2011
Corresponding author: Fei Xiao (fxiao316@gmail.com).

and low-cost integration. A high-performance planar microwave filter is usually required to have good selectivity, good attenuation level in rejection bands and sufficiently wide upper stopband [1]. $\lambda/2$ uniform impedance resonators are widely used in designing filters, such as parallel-coupled-line filters [2], open-loop coupled-resonator filters [3], etc. Additionally, $\lambda/4$ uniform impedance resonators that can possess higher-order harmonics are discussed in [4]. Recently, the stepped-impedance resonator filter has been very popular due to its ability to reduce the circuit size and to improve the upper stopband performance [5, 6]. Some hybrid filter structures, by combing both $\lambda/2$ and $\lambda/4$ resonator, have been proposed in [7, 8].

In this paper, a novel hybrid third-order filter structure based on one $\lambda/2$ and two $\lambda/4$ uniform impedance resonators and capable of realizing a triplet coupling scheme is proposed. The analysis and design of its circuit model is described in detail. The simulation shows that there is a transmission zero located at the low side of its passband. In addition, it can achieve good selectivity and spurious harmonic suppression. Further, the source/load coupling can be introduced to create more transmission zeros; this makes its performance flexible in practice. To verify our analysis, three microstrip filters based on such circuit model are designed, fabricated and measured, respectively. Both simulation and experiment verify the analysis.

2. THE PROPOSED FILTER WITHOUT THE SOURCE/LOAD COUPLING AND ITS EQUIVALENT CIRCUIT ANALYSIS

In Figure 1, the layout of the proposed third-order filter structure is presented. Without metallic via hole, such structure is only two uniform impedance resonators. The via hole, having the radius r (see Figure 1), split the low $\lambda/2$ uniform impedance resonator into two $\lambda/4$ uniform impedance resonators; this also serves as an impedance inverter between these two $\lambda/4$ resonators. Suppose that the signal from the input port is coupled through the gap d_1 into the left $\lambda/4$ uniform impedance resonator and the signal is then split into two. One is coupled to another $\lambda/4$ uniform impedance resonator through magnetic coupling meanwhile the other is coupled to the upper $\lambda/2$ uniform impedance resonator through electrical coupling. When reaching the output port, the signals might cancel each other out to create one transmission zero or more. Therefore, such filter structure can be called as the triplet coupling scheme as usual. To verify our supposition, the I/O ports are weakly coupled to the resonators and then the EM simulation is made. The simulated results are presented

in Figure 2, which shows the modal resonant characteristic of the proposed structure. There are three resonances which correspond to three resonators in our structure. By changing l_2, i.e., the length of the upper $\lambda/2$ resonator, the lowest modal resonance frequency will move upwards or downwards, which means that it corresponds to the upper $\lambda/2$ resonator while the other two correspond to the low two $\lambda/4$ resonators. Correspondingly, the bandwidth can be adjusted. By the way, the observed transmission zero is tightly associated with the lowest modal resonance frequency.

In order to analyze the proposed third-order filter structure, its equivalent circuit model is shown in Figure 3. According to [9], a metallic via hole is equivalent to a grounded inductor having the

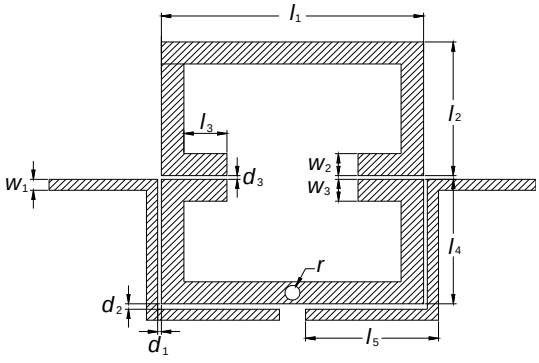

Figure 1. The proposed third-order filter without the source/load coupling.

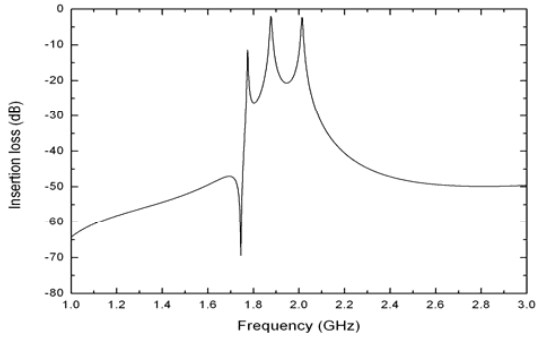

Figure 2. Modal resonant characteristic of the proposed structure.

inductance

$$L = \frac{\mu_0}{2\pi}\left[h \cdot \ln\left(\frac{h+\sqrt{r^2+h^2}}{r}\right) + \frac{3}{2}(r - \sqrt{r^2+h^2})\right] \quad (1)$$

where $h = 0.7\,\text{mm}$ is the via length and r the via radius. For example, if we set $r = 0.4\,\text{mm}$ in our design, $L = 56\,\text{pH}$.

As we can see, there are two signal paths. When signal is input into Port 1 or Port 2, it will go through these two paths separately and finally combine to reach Port 2 or Port 1. In some sense, they might cancel each other at some frequencies, which means that transmission zeros might be created. As is known, appropriate transmission zeros might help to achieve better selectivity and suppression of harmonics.

For simplicity, we choose the same width for all transmission lines in Figure 3 and neglect bending loss, etc. Roughly speaking, the circuit model in Figure 3 is somewhat difficult to be analyzed directly. We can introduce some equivalent circuits to simplify some components in Figure 3 further. For example, in [10–13], the equivalent circuit diagram of a three-port coupled microstrip line section is derived, which is presented in Figure 4, where

$$s = j\tan\theta \quad (2)$$

$$Y_{c0} = s\frac{Y_{0o}+Y_{0e}}{2} \quad (3)$$

$$n = \frac{Y_{0o}+Y_{0e}}{Y_{0o}-Y_{0e}} \quad (4)$$

$$Y_{c1} = \frac{2Y_{0o}Y_{0e}}{Y_{0o}+Y_{0e}} \quad (5)$$

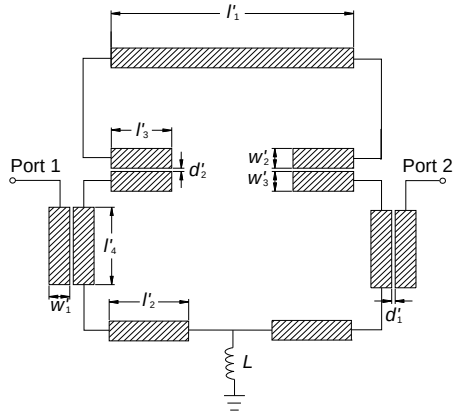

Figure 3. Circuit model of the proposed filter.

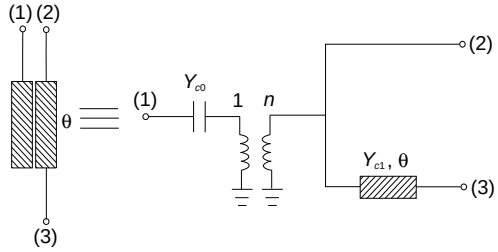

Figure 4. Equivalent circuit diagram of a three-port coupled line section.

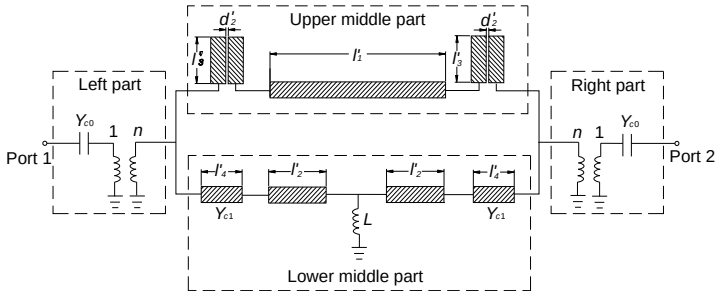

Figure 5. Simplified equivalent circuit diagram of the proposed filter.

Y_{0e} and Y_{0o} are the even- and odd-mode characteristic admittance of the coupled transmission lines respectively, and θ the electrical length of the coupled microstrip line sections. The method for computing these parameters can be found in various handbooks such as [14, 15].

The simplified equivalent circuit of the proposed filter is presented in Figure 5. For analysis, the circuit is divided into four parts, for which the transmission matrices are derived separately; it is then cascaded to get the scattering matrix of the whole circuit model. For a reciprocal two-port network, the transmission matrix has the general property that the determinant $AD - BC = 1$. If, in addition, the network is symmetrical, the diagonal elements are equal, i.e., $A = D$. First, let's consider the left circuit part, including a series capacitor and a transformer. The transmission matrix is

$$[T_L] = [T'_L] \cdot [T''_L] \tag{6}$$

where $[T'_L]$ is the transmission matrix of the series capacitor Y_{c0} and $[T''_L]$ that of the transformer, resulting in

$$[T_L] = \begin{bmatrix} \frac{Y_{0o}-Y_{0e}}{Y_{0o}+Y_{0e}} & \frac{2}{j\tan\theta'_4(Y_{0o}-Y_{0e})} \\ 0 & \frac{Y_{0o}+Y_{0e}}{Y_{0o}-Y_{0e}} \end{bmatrix} \tag{7}$$

The right circuit part obtain

$$[T_R] = [T'_R] \cdot [T''_R] \tag{8}$$

where $[T'_R]$ is the transmission matrix of the transformer and $[T''_R]$ that of the series capacitor Y_{c0}, resulting in

$$[T_R] = \begin{bmatrix} \frac{Y_{0o}+Y_{0e}}{Y_{0o}-Y_{0e}} & \frac{2}{j\tan\theta'_4(Y_{0o}-Y_{0e})} \\ 0 & \frac{Y_{0o}-Y_{0e}}{Y_{0o}+Y_{0e}} \end{bmatrix} \tag{9}$$

The symmetrical upper middle circuit part includes two pairs of coupled transmission lines sections with two open-circuited ports and a transmission line section with the length of l_3. Its transmission matrix is

$$[T_{mu}] = [T'_{mu}] \cdot [T''_{mu}] \cdot [T'_{mu}] \tag{10}$$

where $[T'_{mu}]$ is the transmission matrix of the coupled transmission lines with two open-circuited ports, i.e.,

$$[T'_{mu}] = \begin{bmatrix} \frac{Z_{0e}+Z_{0o}}{Z_{0e}-Z_{0o}} & -j\cot\theta'_3 \cdot \frac{2Z_{0e}Z_{0o}}{Z_{0e}-Z_{0o}} \\ j\tan\theta'_3 \cdot \frac{2}{Z_{0e}-Z_{0o}} & \frac{Z_{0e}+Z_{0o}}{Z_{0e}-Z_{0o}} \end{bmatrix} \tag{11}$$

$[T''_{mu}]$ is that of the single transmission line section with the length of l_3, i.e.,

$$[T''_{mu}] = \begin{bmatrix} \cos\theta'_1 & jZ_c\sin\theta'_1 \\ \frac{j}{Z_c}\sin\theta'_1 & \cos\theta'_1 \end{bmatrix} \tag{12}$$

We can substitute these expressions by including (11) and (12) into (10) and simplify it. For simplicity, the final result is not given here.

The symmetrical lower middle circuit part includes four transmission line sections and a shunt inductor, L. We can also derive the transmission matrix of this circuit part as follows

$$[T_{md}] = [T'_{md}] \cdot [T''_{md}] \cdot [T'''_{md}] \cdot [T''_{md}] \cdot [T'_{md}] \tag{13}$$

where $[T'_{md}]$ is the transmission matrix of the single transmission line section with the length of l'_4 and the characteristic admittance of Y_{c1}, $[T''_{md}]$, that of the single transmission line section with the length of l'_2, and $[T'''_{md}]$ that of the shunt inductor L.

We can then transform $[T_{mu}]$ into the corresponding admittance matrix $[Y_{mu}]$ and $[T_{md}]$ into $[Y_{md}]$ in the similar way respectively. We add them to get

$$[Y_m] = [Y_{mu}] + [Y_{md}] \tag{14}$$

which has the property $Y^m_{11} = Y^m_{22}$ and $Y^m_{12} = Y^m_{21}$. Then, we can obtain the corresponding transmission matrix $[T_m]$ from $[Y_m]$.

By cascading the three transmission matrices, i.e., T_L, T_m and T_R, we obtain the transmission matrix of the whole equivalent circuit shown in Figure 5.

$$[T] = [T_L] \cdot [T_m] \cdot [T_R] \tag{15}$$

Finally, we obtain the scattering matrix $[S]$ from $[T]$ for the entire network, which is reciprocal and symmetrical.

The design of this type of filter can follow the design procedure of trisection structure described in [1, 16, 17]. Firstly, according to specifications, the unknown element values of a lowpass prototype filter may be determined by a synthesis method or through an optimization process [16]. Then, the resonant frequencies, the external quality factors and the coupling coefficients for microstrip implementation can be found through the following equations.

$$\omega_{0i} = \frac{1}{\sqrt{L_i C_i}} = \omega_0 \sqrt{1 - \frac{B_i}{g_i/FBW + B_i/2}} \tag{16}$$

$$Q_{e1} = \frac{b_1}{g_0} = \frac{\omega_{0i}}{\omega_0 g_0} \left(\frac{g_1}{FBW} + \frac{B_1}{2} \right) \tag{17}$$

$$Q_{en} = \frac{b_n}{g_{n+1}} = \frac{\omega_{0n}}{\omega_0 g_{n+1}} \left(\frac{g_n}{FBW} + \frac{B_n}{2} \right) \tag{18}$$

$$\begin{aligned} M_{ij}|_{i \neq j} &= \frac{J_{ij}}{\sqrt{b_i b_j}} \\ &= \frac{\omega_0}{\sqrt{\omega_{0i}\omega_{0j}}} \frac{FBW \cdot J_{ij}}{\sqrt{(g_i + FBW \cdot B_i/2) \cdot (g_i + FBW \cdot B_j/2)}} \end{aligned} \tag{19}$$

where ω_0 is the midband frequency and FBW is the fractional bandwidth of the bandpass filter.

Once these parameters are obtained, the initial dimensions of the filter can be determined and then we can optimize the performance of the filter through the EM optimization. For example, we design a microwave filter whose center frequency is 1.94 GHz and fractional bandwidth 5.3%. A 0.635-mm-thick dielectric substrate, with a relative dielectric constant of 9.5, is chosen. In addition, $l'_1 = 25.3\,\text{mm}$, $l'_2 = 1.1\,\text{mm}$, $l'_3 = 2.3\,\text{mm}$, $l'_4 = 11.2\,\text{mm}$, $d'_1 = d'_2 = 0.2\,\text{mm}$, $w'_1 = w'_2 = w'_3 = 1.2\,\text{mm}$, $L = 56\,\text{pH}$. The frequency response of the proposed filter simulated by both Matlab and HFSS is presented in Figure 6. In the lower stopband, there is a transmission zero whose location can be computed by setting $S_{21} = 0$. In a word, both EM and circuit simulations verify our supposition that our proposed structure consists of one $\lambda/2$ and two $\lambda/4$ uniform impedance resonators. To design this type of the filter, these three modal frequencies should be

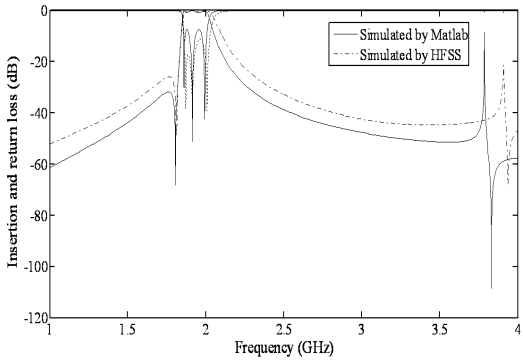

Figure 6. Frequency response of the circuit model of the proposed filter simulated by Matlab and HFSS.

allocated into the desired passband. For a given center frequency, the perimeter of the $\lambda/2$ and two $\lambda/4$ resonators can be determined by it and then tuned to the desired values.

3. MICROSTRIP REALIZATION OF THE PROPOSED THIRD-ORDER FILTER WITHOUT SOURCE/LOAD COUPLING

To verify our concept, we realize our first microstrip filter according to Figure 1. The center frequency of the filter is set at 1.94 GHz, with the factional bandwidth of 8.3%. We chose $w_1 = 0.3$ mm for the width of the input and output microstrip for impedance matching with the outside system. In addition, it could increase the coupling strength between the feedlines and the filter to reduce insertion loss. The other structure parameters are set to: $w_2 = w_3 = 1.2$ mm, $l_1 = 14.0$ mm, $l_2 = 7.3$ mm, $l_3 = 2.3$ mm, $l_4 = 6.8$ mm, $l_5 = 7.1$ mm, $d_1 = 0.2$ mm, $d_2 = 0.3$ mm, $d_3 = 0.2$ mm, and $r = 0.4$ mm.

Next, the microstrip filter is fabricated (see the photograph in Figure 7). The size of the filter is only $0.243\lambda_g \times 0.248\lambda_g$, where λ_g is the microstrip guide wavelength at 1.94 GHz. The electromagnetic simulation is done by HFSS and the frequency response of the filter is measured by Angilent network analyzer. The simulated and measured frequency responses of the filter are presented in Figure 8 and the results agree well. The measured center frequency is 1.97 GHz and the measured fractional bandwidth 6.5%. The frequency shift might be unexpected tolerance in fabrication and material parameters. The insertion loss including the SMA connector loss is about 1.9 dB. The return loss in the passband is less than -9.5 dB. The return loss might

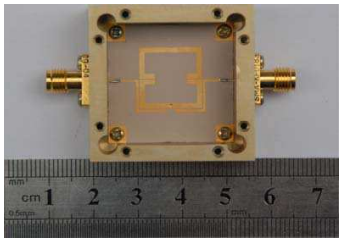

Figure 7. The photograph of the fabricated filter.

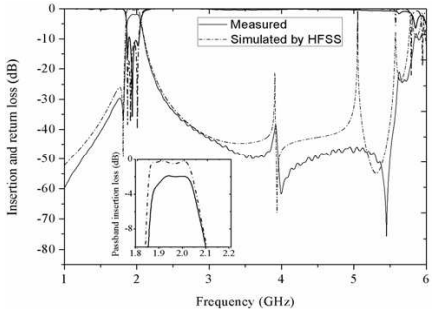

Figure 8. Simulated and measured frequency response of the proposed filter.

be reduced further, if the rectangular bends in the filter structure are smoothed to reduce reflection. We can observe that there is one transmission zero right below the passband. Aside from its advantage of good selectivity, this filter performs very well at harmonic suppression. About 40 dB harmonic suppression can be achieved from about 2.5 GHz to 5.5 GHz.

4. MICROSTRIP REALIZATION OF THE PROPOSED FILTER WITH SOURCE/LOAD COUPLING

In the previous section, a microstrip filter without the source/load coupling was discussed. There is a transmission zero located at the low side of the passband. In this section, we consider our second design, featuring the addition of the source/load coupling. The layout of the filter with the source/load coupling is presented in Figure 9. While keeping other parameters unchanged, we chose $l_6 = 0.6$ mm, $w_4 = 0.5$ mm, and $d_4 = 0.2$ mm. As is well known, two microstrip lines with a gap between their open ends can be modeled by a series capacitor, thus creating electrical coupling between the two open ends. In this way, a more direct signal path is introduced between the input and output terminals.

The photograph of the fabricated filter is shown in Figure 10. The simulated and measured frequency responses of the filter are presented in Figure 11. Compared with these of the filter without the source/load coupling, the passband of the filter with source/load coupling almost keeps unchanged. The insertion loss, including the SMA connector loss, is about 1.8 dB. The return loss in the passband is less than -9.6 dB. As an effect of the source/load coupling, however we can

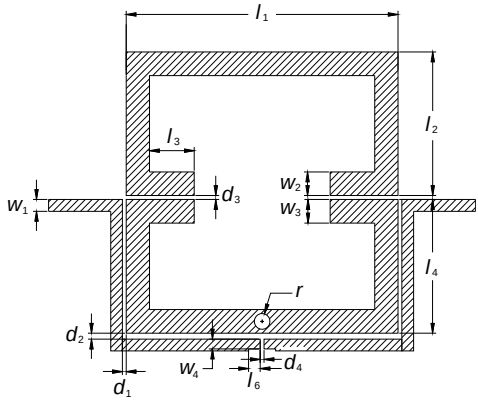

Figure 9. Microstrip realization of the our second filter design with source/load coupling.

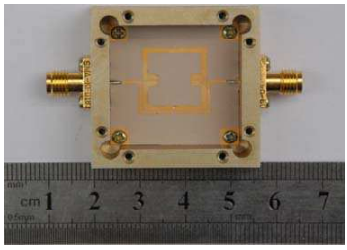

Figure 10. The photograph of the fabricated filter.

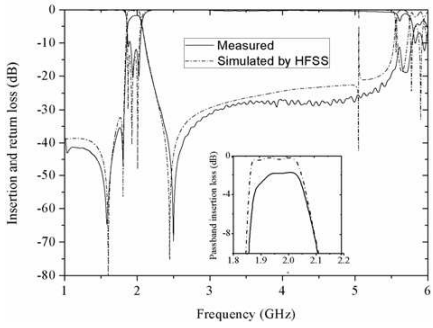

Figure 11. Simulated and measured frequency response of our second filter design.

now observe that there are in total three transmission zeros: two at 1.58 GHz, 1.81 GHz in the lower stopband and one at 2.50 GHz in the upper stopband. This verifies that our filter structure can realize the triplet coupling scheme. Although harmonic suppression of the filter with the source/load coupling seems to not be better than that of the filter without the source/load coupling, it still can achieve about 30 dB harmonic suppression from about 2.5 GHz to 5.5 GHz.

5. MICROSTRIP REALIZATION OF THE PROPOSED FILTER WITH SOURCE/LOAD COUPLING WITH EXTENSIONS

In [18], several second-order filters, using coupled lines with loads at one end, are discussed. The analysis shows that coupled lines with load at one end might create one transmission zero or more. In this section, we use a pair of coupled transmission line with the stubs as source/load coupling for our third filter design. The electromagnetic simulation verifies that such structure can introduce a new transmission zero in the upper frequency range of the filter, which might be used to suppress specific harmonic. In addition, this transmission zero can be moved downward or upward by only changing the length of the stubs without affecting the passband. It is therefore very flexible.

The layout of our third filter design is shown in Figure 12. Compared with the two filters in the previous sections, there is no difference except that a pair of coupled transmission lines with the stubs are attached source/load coupling. Without changing other structure parameters, we set $d_4 = 0.2\,\text{mm}$ and $l_7 = 2.0\,\text{mm}$. To inspect the effect of the length l on the new transmission zero, electromagnetic simulations using HFSS are done. In Figure 13, the simulated frequency response of the proposed filter, with different value of the length l, is presented. Obviously, there is a new transmission zero in the upper frequency range. If the length l is changed, this transmission zero will be moved downward or upward, accordingly. Interestingly, the change in the length l seems to have no effect on the performance of the passband. In order to verify our supposition, we do an additional HFSS simulation for the source/load coupling structure

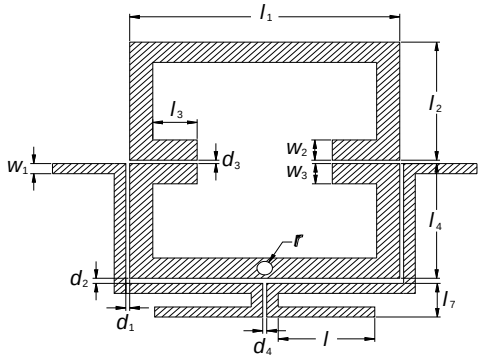

Figure 12. Microstrip realization of the third filter design with source/load coupling with extensions.

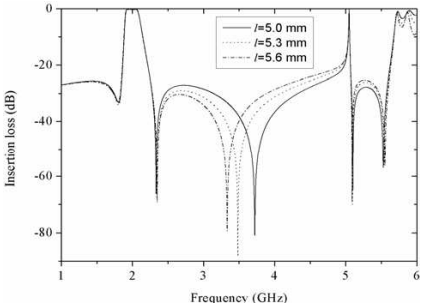

Figure 13. Simulated frequency response of the third filter design for different values of the extension length l.

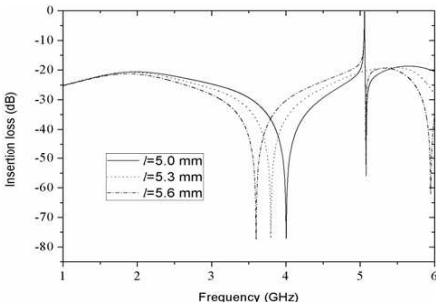

Figure 14. Simulated frequency response of the source/load coupling structure with different values of the length l.

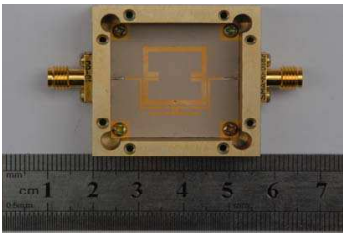

Figure 15. The photograph of the fabricated filter design 3, where the extensions have the length of $l = 5.0\,\mathrm{mm}$.

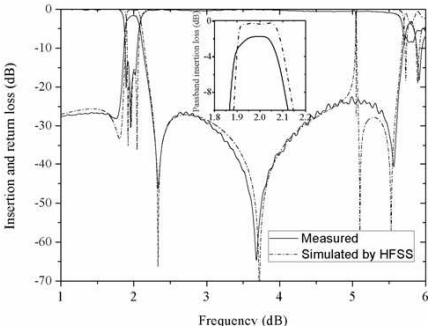

Figure 16. Simulated and measured frequency response of the filter design 3.

with extensions only, i.e., without any resonators present. In Figure 14, the electromagnetic simulation results show that such source/load coupling structure with extensions creates one transmission zero in the desired position; additionally, the length of the extensions have minor influence at the passband frequencies.

The filter fabricated from the layout in Figure 12 is realized with extensions having the length $l = 5.0\,\mathrm{mm}$: see the photograph in Figure 15. The simulated and measured frequency responses of the filter are shown in Figure 16. The results agree very well and we can observe the new transmission zero in the upper frequency range. By changing the length of the stubs, i.e., l, this transmission zero could

be moved to the desired location, which might be used to suppress undesired harmonics.

6. CONCLUSION

In this paper, a novel microwave third-order filter structure has been proposed and analyzed. Based on such analysis, three different microstrip bandpass filters have been designed, fabricated and measured. One or more transmission zeros can be created for these filters. Our simulated and measured results show that these compact filters have good selectivity and suppression of spurious harmonics.

ACKNOWLEDGMENT

This work was supported in part by the National Science Foundation for Young Scientists of China under Grant No. 60801028, CSC (Chinese Scholar Council), and the Swedish Research Council (VR) (No. 2006-4048).

REFERENCES

1. Hong, J.-S. and M. J. Lancaster, *Microstrip Filters for RF/Microwave Applications*, Wiley, New York, 2001.
2. Cohn, S. B., "Parallel-coupled transmission-line-resonator filters," *IEEE Trans. Microw. Theory Tech.*, Vol. 6, No. 2, 223–231, Apr. 1958.
3. Hong, J.-S. and M. J. Lancaster, "Cross-coupled microstrip hairpin-resonator filters," *IEEE Trans. Microw. Theory Tech.*, Vol. 46, No. 1, 118–122, Jan. 1998.
4. Matthaei, G. L., "Interdigital bandpass filter," *IRE Trans. Microw. Theory Tech.*, Vol. 10, No. 6, 41–45, Nov. 1962.
5. Makimoto, M. and S. Yamashita, "Bandpass filters using parallel coupled stripline stepped impedance resonators," *IEEE Trans. Microw. Theory Tech.*, Vol. 28, No. 12, 1413–1417, Dec. 1980.
6. Chen, C. C., Y. R. Chen, and C. Y. Chang, "Miniaturized microstrip cross-coupled filters using quarter-wave or quasi-quarter-wave resonators," *IEEE Trans. Microw. Theory Tech.*, Vol. 51, No. 1, 120–131, Jan. 2003.
7. Lin, S. C., Y. S. Lin, and C. H. Chen, "Extended-stopband bandpass filter using both half- and quarter-wavelength resonators," *IEEE Microw. Wireless Compon. Lett.*, Vol. 16, No. 1, 43–45, Jan. 2006.

8. Deng, P. H., C. H. Wang, and C. H. Chen, "Novel broadside-coupled bandpass filters using both microstrip and coplanar-waveguide resonators," *IEEE Trans. Microw. Theory Tech.*, Vol. 54, No. 10, 3746–3750, Oct. 2006.
9. Goldfarb, M. E. and R. A. Pucel, "Modeling via hole grounds in microstrip," *IEEE Microwave Guided Wave Lett.*, Vol. 1, No. 6, 135–137, Jun. 1991.
10. Sato, R. and E. G. Cristal, "Simplified analysis of coupled transmission ine networks," *IEEE Trans. Microw. Theory Tech.*, Vol. 18, No. 3, 122–131, Mar. 1970.
11. Nemoto, Y., K. Kobayashi, and R. Sato, "Graph transformations of nonuniform coupled transmission line networks and their application," *IEEE Trans. Microw. Theory Tech.*, Vol. 33, No. 11, 1257–1263, Nov. 1985.
12. Ozaki, H. and J. Ishii, "Synthesis of a class of strip-line filters," *IRE Trans. Circuit Theory*, Vol. 5, No. 2, 104–109, Jun. 1958.
13. Mohd Salleh, M. K., G. Prigent, O. Pigaglio, and R. Crampagne, "Quarter-wavelength side-coupled ring resonator for bandpass filters," *IEEE Trans. Microw. Theory Tech.*, Vol. 56, No. 1, 156–162, Jan. 2008.
14. Wadell, B. C., *Transmission Line Design Handbook*, Norwood, USA, 1991.
15. Rosloniec, S., *Algorithms for Computer-aided Design of Linear Microwave Circuits*, Norwood, USA, 1990.
16. Hunter, I., "Theory and design of microwave filters," *IEE Electromagnetic Waves Series*, 2001.
17. Ismail, A., M. S. Razalli, M. A. Mahdi, R. S. A. Raja Abdullah, N. K. Noordin, and M. F. A Rasid, "X-band trisection substrate-integrated waveguide quasi-elliptic filter," *Progress In Electromagnetics Research*, Vol. 85, 133–145, 2008.
18. Tsai, C. M., S. Y. Lee, and H. M. Lee, "Transmission-line filters with capacitively loaded coupled lines," *IEEE Trans. Microw. Theory Tech.*, Vol. 51, No. 5, 1517–1524, May 2003.